A Gas Hydrate System of Heterogeneous Character in the Nile Deep-Sea Fan

Daniel Praeg, Sébastien Migeon, Jean Mascle, Vikram Unnithan, Marcelo Ketzer

A Gas Hydrate System of Heterogeneous Character in the Nile Deep-Sea Fan

37

Daniel Praeg, Sébastien Migeon, Jean Mascle, Vikram Unnithan, and Marcelo Ketzer

Abstract

Large deep-sea fans are useful settings to study gas hydrate systems, the rapid burial of organic-rich sediment driving linked processes of gas generation, fluid expulsion and syn-sedimentary tectonism. The Nile deep-sea fan (100,000 km^2) is a collapsing Late Cenozoic depocentre that is both a hydrocarbon province and an area of widespread seafloor fluid seepage. Evidence for gas hydrates has been reported in this area, but remains poorly documented. Available seismic and well data are used together with information on seafloor features to characterise a deep-water (1500–2700 m) gas hydrate system in the central Nile fan. The system is in part expressed as a bottom simulating reflection (BSR) discontinuously observed across a relatively small area (6000 km^2), both cross-cutting the stratified fill of fault-bound slope basins, and upslope of the basins within thick unstratified mass transport deposits. West of the BSR area, log data from two wells 45 km apart indicate the presence of gas hydrates in intervals up to 75 m thick near the base of the stability zone. Gas hydrates are also likely to be present near the seafloor within hundreds of pockmark-like mounds that record gas venting through the stability zone, most observed west of the BSR area. The central Nile fan thus contains a gas hydrate system expressed as two areas of comparable size, one with a discontinuous BSR but few seafloor gas vents, another lacking a BSR but with downhole evidence of gas hydrates and abundant gas venting. This heterogenous character is suggested to reflect spatial variations in fluid expulsion from the Nile fan, which can inhibit BSR formation while favouring gas hydrate accumulation over wide areas. This possibility has implications for other large deep-sea fans, many of which have restricted BSRs but may contain more extensive gas hydrate systems.

D. Praeg (✉) · S. Migeon
Géoazur (CNRS UMR7329), 250 Rue Albert Einstein, 06560 Valbonne, France
e-mail: praeg@geoazur.unice.fr

J. Mascle
Villefranche Oceanographic Observatory, Port de la Darse, 06230 Villefranche-sur-Mer, France

V. Unnithan
Department of Physics and Earth Sciences, Jacobs University Bremen, Campus Ring 1, 28759 Bremen, Germany

M. Ketzer
Department of Biology and Environmental Science, Linnaeus University, 391 82 Kalmar, Sweden

37.1 Introduction

The submarine fans of large rivers are Earth's primary locations for long-term carbon burial (Leithold et al. 2016) and provide ideal conditions for the accumulation of gas hydrates, rapid deposition favoring gas generation by biogenic and thermogenic processes, as well as pore fluid expulsion through the hydrate stability zone (Gornitz and Fung 1994). Fluid migration to the seafloor may be facilitated by syn-sedimentary fault systems that develop in response to gravitational collapse above deep décollements (e.g., Morley et al. 2011; Ketzer et al. 2018). An upward flow of gas-rich fluid has broad implications for gas hydrate systems, as it has been shown to result in higher concentrations of hydrates (Hornbach et al. 2012) and may contribute to the appearance of bottom simulating reflectors (BSRs; Haacke et al. 2007) as well as to the development of chimney-like structures that vent fluids to the seafloor through the stability zone (Liu and Fleming 2007; Haacke et al. 2009; Riedel et al. 2010).

The Nile is the world's longest river, culminating in a submarine fan (Fig. 37.1) at least 3 km thick that forms the largest post-Messinian depocenter in the Mediterranean Sea (Gennessaux et al. 1998; Loncke et al. 2006). The Nile deep-sea fan forms the upper part of a post-rift succession at least 7 km thick on the Egyptian margin (Abdel et al. 2000, 2001; Camera et al. 2010), which has undergone multi-stage

J. Mienert et al. (eds.), *World Atlas of Submarine Gas Hydrates in Continental Margins*,
https://doi.org/10.1007/978-3-030-81186-0_37

gravitational collapse above décollements at two levels: shales of Upper Cretaceous to Eocene age and Messinian evaporites (Morley et al. 2011; Tassy et al. 2015). The succession contains giant gas reservoirs from the Oligocene to Pleistocene, recording upward hydrocarbon migration from deeper thermogenic sources, mixing at shallower levels with methane of microbial origin (Abdel et al. 2000; Dolson et al. 2005; Vandré et al. 2007). Widespread fluid seepage is expressed as oil slicks above major faults (Abdel et al. 2000, 2001) and as seafloor features including mud volcanoes and pockmark-like fluid seeps (Fig. 37.1; Loncke et al. 2002, 2004; Mascle et al. 2005; Bayon et al. 2009b; Dupré et al. 2010; Römer et al. 2014). Geochemical studies reveal that the mud volcanoes emit gas of both thermogenic and microbial origin (Prinzhofer and Deville 2013), whereas the pockmark-like features release nearly-pure methane (Bayon et al. 2009b; Römer et al. 2014) from areas of authigenic carbonates that are isotopically consistent with the anaerobic oxidation of microbially-derived methane (Gontharet et al. 2007).

Gas hydrates have been sampled from mud volcanoes in the Anaximander Mountains of the Mediterranean Sea, within the Africa-Eurasia accretionary complex north of the Nile fan (Fig. 37.1 inset; Lykousis et al. 2009; Pape et al. 2010). A recent review of gas hydrates offshore Europe (Minshull et al. 2020) found that, despite the wide distribution of seismic reflection data in the eastern Mediterranean Sea, evidence of a BSR was limited to a single profile across the central Nile fan offshore Egypt (Praeg et al. 2008) and to scattered 3D seismic amplitude anomalies in the eastern Nile fan off Israel proposed to represent a 'pseudo-BSR' (Tayber et al. 2019). However, geophysical evidence of gas hydrates has been recognized for 20 years by the Egyptian exploration industry, albeit based on seismic and well data that remain poorly documented. The presence of gas hydrates was first noted based on 2D/3D seismic data from Shell's NEMed deepwater concession (Fig. 37.1; Abdel et al. 2000, 2001), which revealed a BSR at water depths below 1800 m (Nott et al. 2001). Examples of the BSR subsequently appeared in an unpublished thesis (Newton 2006) and in

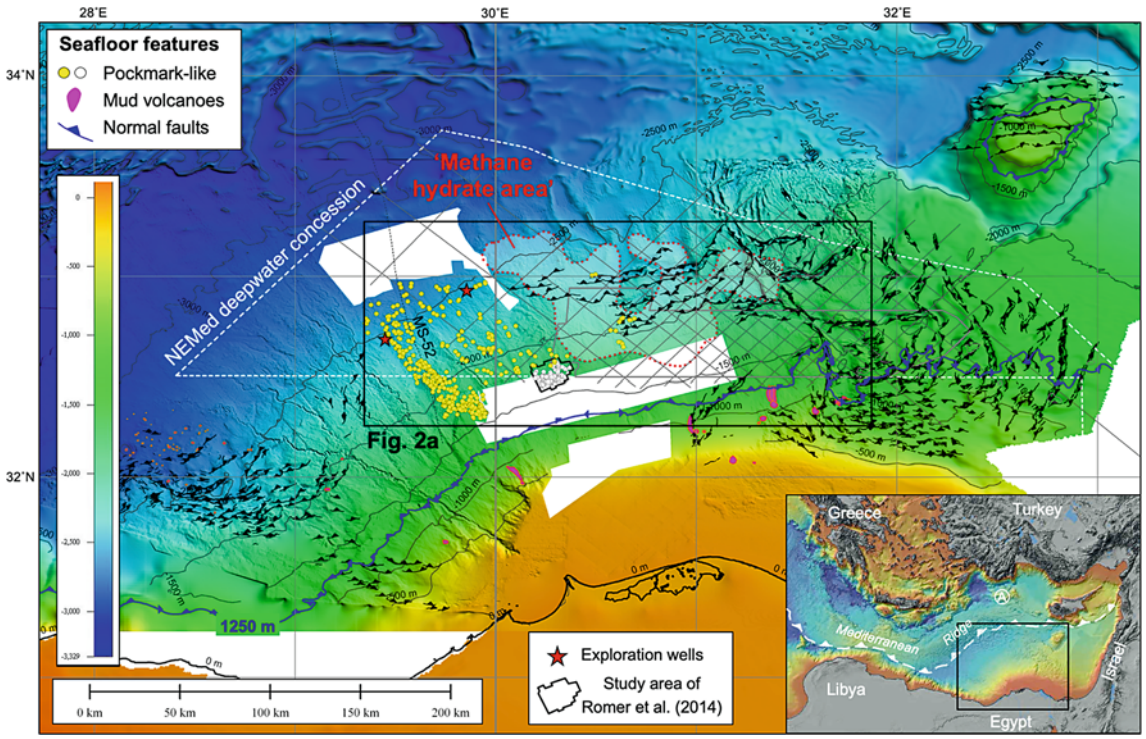

Fig. 37.1 Location of the Nile deep-sea fan showing seafloor bathymetry based on a regional multibeam mosaic (acquired by Géoazur from 1998 to 2011) used to map the indicated seafloor features. 'Pockmark-like' features refer to reflective carbonate patches 75–400 m wide of mainly positive relief (yellow dots identified for this study, white dots from the study of Römer et al. 2014). The 1250 m bathymetric contour (highlighted in blue) corresponds to the approximate upper limit of the methane hydrate stability zone. The possible extent of a BSR within the NEMed deepwater concession is indicated by a 'methane hydrate area' taken from a Shell concession map (Sharaf El Din 2006). Exploration 2D and 3D seismic data available to this study are shown by the grey lines and polygon, dotted line indicates OGS profile MS-52. Red stars indicate the locations of two exploration wells (see Figs. 37.2a, 37.4). Inset: dashed line with arrows indicates the southern limit of the Africa-Eurasia accretionary system (from Mascle and Mascle 2012); circle marked A indicates the location of the Anaximander Mountains where gas hydrates have been sampled in mud volcanoes (see text)

conference presentations (Sharaf El Din 2006; Sharaf El Din and Nassar 2010). The possible extent of the BSR relative to the NEMed seismic data was suggested by a 'methane hydrate area' on a Shell concession map (Sharaf El Din 2006), reproduced in Fig. 37.1. In addition, downhole evidence of gas hydrates has been reported in two Shell wells 'in deepwater North Africa' (Nimblett et al. 2005), here shown to lie on the central Nile fan within the NEMed concession (Fig. 37.1).

This article documents evidence for a gas hydrate system in the central Nile fan using exploration seismic and well data as well as morpho-bathymetric data on seafloor features (Fig. 37.1). 2D/3D seismic data are first used to verify the occurrence of a BSR within the NEMed concession (Figs. 37.2, 37.3). Two wells presented by Nimblett et al. (2005) are then shown to provide evidence of gas hydrates with the area of the BSR (Fig. 37.4). Finally, indicators for fluid seeps within the hydrate stability zone are shown (Fig. 37.5). The results provide an example of a heterogeneous deep-water gas hydrate system that is only in part expressed by a BSR and is associated with widespread gas venting to the ocean.

37.2 Regional Setting

The Nile deep-sea fan extends over an area of 100,000 km^2, reaching up to 250 km from the Egyptian coast and into water depths of up to 3000 m (Fig. 37.1). Its seafloor morphology has been described using multibeam data and is divided into western, central and eastern provinces (Fig. 37.1; Loncke et al. 2002, 2004). Extensional fault systems resulting mainly from Messinian salt withdrawal are present in the western and eastern provinces; they also extend across the north of the central province, where they form a series of slope-parallel basins at water depths of 2000–2400 m (Figs. 37.1, 37.2). In contrast, most of the central province upslope of the faults features un-deformed sediment deposited on a stable pre-Messinian platform, where mobile evaporites were not deposited (Loncke et al. 2004 2006).

The post-Messinian succession of the Nile fan consists of turbiditic facies interbedded with giant mass-transport deposits (MTDs) up to 300 m thick (Loncke et al. 2009; Migeon et al. 2014; Omeru and Cartwright 2015). The succession is pierced in places by mud volcanoes rooted in pre-Messinian successions (Loncke et al. 2004; Dupré et al. 2010; Prinzhofer and Deville 2013). The central province also contains hundreds of seafloor features that have been referred to as pockmarks but are of mainly positive relief. These are recognized on sonar data as high-backscatter patches up to 400 m wide, which in situ studies show correspond to areas of fractured authigenic carbonate hosting chemosynthetic ecosystems (Loncke et al. 2002, 2004; Bayon et al. 2009a; Dupré et al. 2010; Römer et al. 2014). Dating of the carbonates indicates that they have precipitated over thousands of years (Bayon et al. 2009a, b), while on-going gas venting to the water column is recognised in places from hydroacoustic imagery (Dupré et al. 2010; Praeg et al. 2014; Dano et al. 2014). A detailed hydroacoustic survey of a 225 km^2 area identified 163 features (Fig. 37.1, white dots), all of positive relief of the 163, 8% show vent streams of hydrate-coated methane bubbles, rising to water depths of 1400 m close to the top of the hydrate stability zone (see Fig. 37.5; Römer et al. 2014).

The semi-enclosed Mediterranean Sea is characterized by bottom waters that are unusually warm (12.5–14 °C), leading to a methane hydrate stability zone (MHSZ) that lies below water depths of 1000 m (Praeg et al. 2011), i.e. at least twice as deep as the typical upper limits of 300–500 m in the open ocean. In the eastern Mediterranean Sea, the upper limit of the MHSZ has been estimated to lie at water depths of 1150–1350 m (Pape et al. 2010; Römer et al. 2014; Tayber et al. 2019). The 1250 m depth contour is marked on Fig. 37.1 and shows that methane hydrates are stable across the Nile deep-sea fan within a deep-water area of about 65,000 km^2.

37.3 Evidence of Gas Hydrates

37.3.1 Bottom Simulating Reflection (BSR)

The presence of a BSR on the central Nile fan is verified using available seismic data from the NEMed concession (Fig. 37.2) acquired in 1999 (Abel et al. 2000, 2001; Nott et al. 2001). The grid of exploration profiles, including two 3D cross-lines, represent only part of the full industry dataset used to suggest a 'methane hydrate area' (Figs. 37.1, 37.2a). The BSR is observed on several profiles within this area and to the south as a discontinuous reflection that extends over a total area of 6000 km^2 at water depths of 1650–2400 m (Fig. 37.2a).

The BSR is most evident where it cross-cuts the stratified infill of a series of fault-bound basins as a reflection of negative polarity, with locally high amplitude but low lateral continuity (Fig. 37.2a–c). The BSR is also observed upslope of the basins (Fig. 37.2a) as a relatively low amplitude reflection of higher continuity within thick unstratified mass transport deposits (MTDs; Fig. 37.2d). The discontinuity of the BSR outside the MTDs and within the basins can be partly attributed to interference with reflections from the stratigraphic succession of the fan, which is both complex and offset by faults (e.g., Fig. 37.2b, c). The BSR also experiences lateral fading due to reductions in amplitude, however, notably within the basins. Interestingly, in these

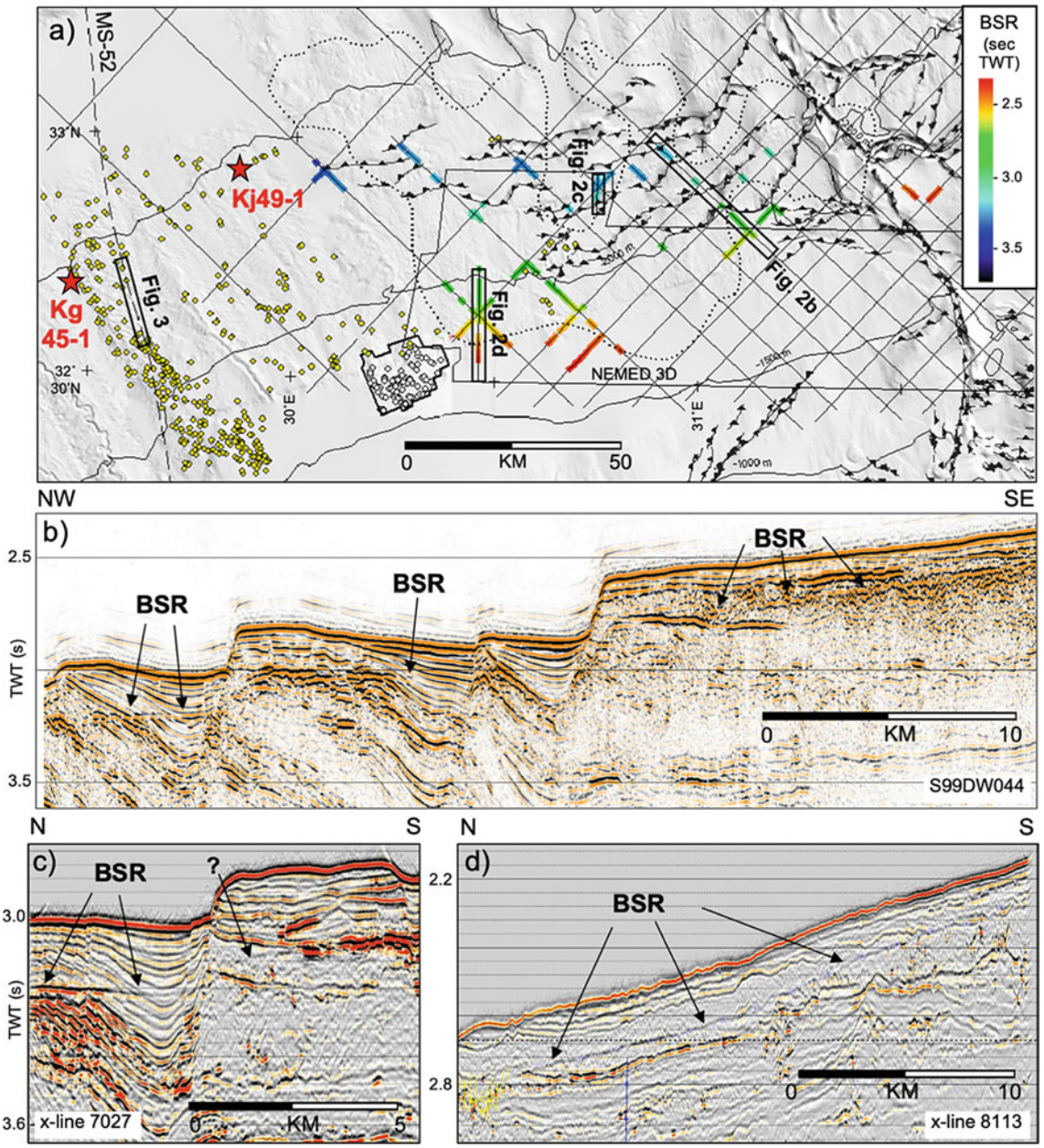

Fig. 37.2 Evidence of a discontinuous gas hydrate BSR on 2D and 3D exploration seismic data: **a** BSR depth observations superimposed on available datasets and seafloor features (see Fig. 37.1; red stars indicate the locations of the two exploration wells shown in Fig. 37.4); **b** and **c** seismic profiles showing a BSR cross-cutting stratified succession within fault-bounded basins, at left, and within unstratified MTDs, at right; note the BSR rising towards seafloor and fading towards the faults; **d** seismic profile showing a more continuous but faint BSR within a thick MTD

areas the BSR does not consistently 'simulate' the relatively flat seafloor of the basins, but in places rises towards seafloor (e.g., Fig. 37.2b, c).

A BSR was also hypothesized by Praeg et al. (2008) along a multichannel seismic profile acquired in 1973 west of the exploration profile grid (MS-52, Figs. 37.1, 37.2a), and has been cited as evidence of gas hydrates by various authors (e.g. Merey and Longinos 2018; Tayber et al. 2019; Minshull et al. (2020). The profile is reproduced in Fig. 37.3 and illustrates the challenge of identifying a BSR relative to the stratigraphy of the fan on lower quality (12-fold) data. The profile includes a reflection of reverse polarity to seafloor (i.e., negative amplitudes) that lies within the depth range of the base of the methane hydrate stability zone as estimated for minimum and maximum sediment velocities (Fig. 37.3). However, the reflection is of low lateral continuity, and does not simulate the irregular seafloor relief; moreover, it coincides with the base of an MTD that

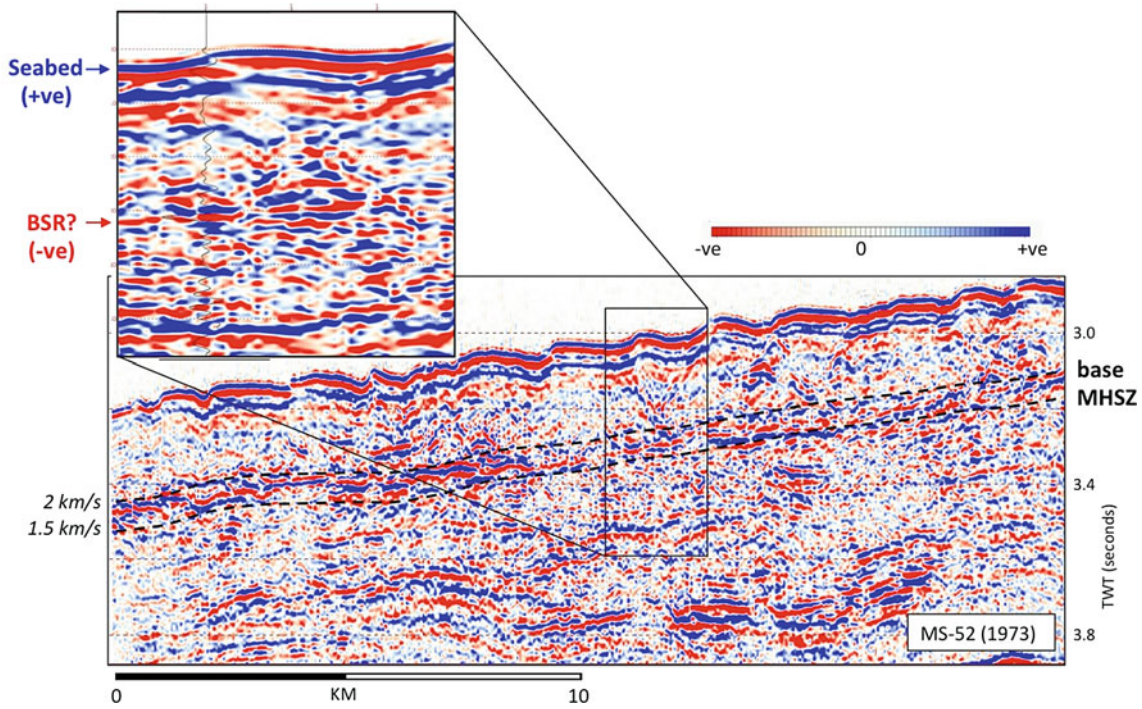

Fig. 37.3 Possible evidence of a BSR on seismic profile MS-52 across the central Nile fan (location in Figs. 37.1, 37.2a), adapted from Praeg et al. (2008). The multichannel profile (12-fold data, 6 km cable) was acquired in 1973 by OGS (Finetti and Morelli 1973). The base of the stability zone for methane hydrates in seawater (base MHSZ) calculated from regional data grids (Praeg et al. 2011) was converted to TWT using minimum and maximum velocities. The two levels bracket a negative amplitude reflection of low continuity that was hypothesized by Praeg et al. (2008) to be a BSR; note that the reflection does not closely mimic seafloor relief and coincides with the base of a thick MTD that could account for an impedance reduction

could account for an impedance reduction (Fig. 37.3). There is no BSR observed on nearby exploration profiles (Fig. 37.2a), even across the sites of two wells (Fig. 37.4; see next section). The profile does not provide conclusive evidence of a BSR; nonetheless, it cannot be excluded that a discontinuous BSR segment is present (Fig. 37.3).

37.3.2 Well Log Data

Downhole evidence of gas hydrates that were not seismically detected prior to drilling was presented by Nimblett et al. (2005) in two exploration wells 'off north Africa', drilled in 2004 in the NEMed concession (Figs. 37.1). The wells were acquired by Shell at locations 45 km apart at water depths of 2443 and 2448 m (Nimblett et al. 2005), allowing them to be identified as Kg45-1 and Kj49-1 (Fig. 37.2a). The presence of gas hydrates was interpreted from high resistivity values in intervals 36–75 m thick, extending from 125 mbsf (i.e., metres below seafloor) down to or near the base of gas hydrate stability (BGHS), estimated for regional conditions to lie at 190 mbsf (Fig. 37.4). Slight gas flows out of the wellhead were detected during drilling and following the emplacement of casing, consistent with the dissociation of gas hydrates (Nimblett et al. 2005).

The high resistivity intervals in both wells lie within 75 m of the BGHS (Fig. 37.4). No seismic indications of gas hydrates were observed at either site (Fig. 37.4). Seismic and well log data indicate the upper 300 m of sediment at these sites is mud-dominated, comprising a thick MTD at Kg45-1, and MTDs interbedded with channel-levee deposits at Kj49-1 (Fig. 37.4; Nimblett et al. 2005). The resistivity log pattern differs in character between the wells, suggesting varying thicknesses and concentrations of gas hydrates (Fig. 37.4). While the wells are located in an area of fluid seeps, they do not coincide with mapped features (Fig. 37.2a) and they would have been carefully positioned to avoid any seafloor or shallow subsurface hazards.

37.3.3 Seafloor Seepage Features

Gas hydrates are also likely to occur in association with fluid seeps that lie within the hydrate stability zone on the Nile fan, as noted in several studies (e.g., Loncke et al. 2004; Mascle et al. 2005; Tayber et al. 2019; Minshull et al. 2020).

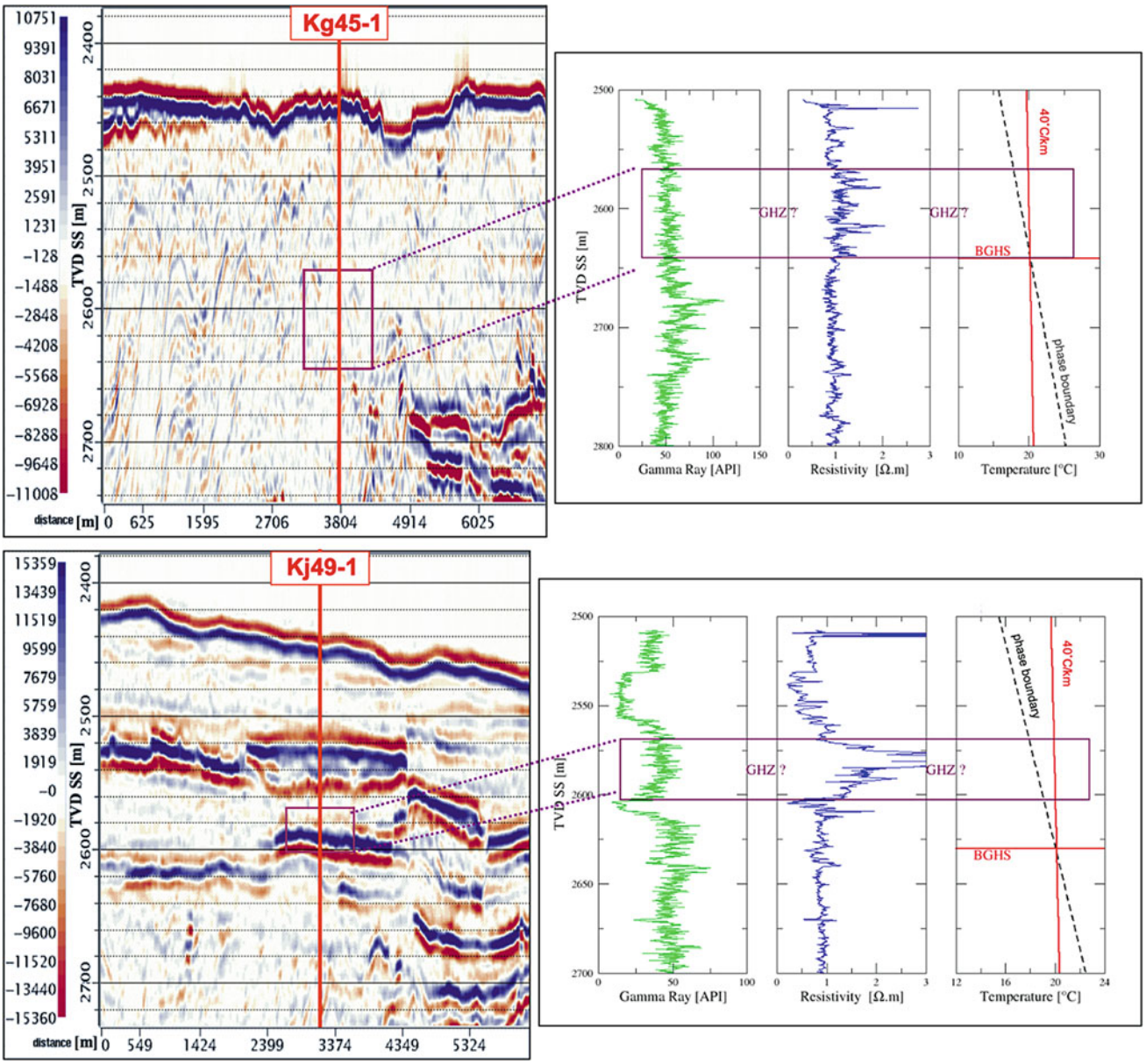

Fig. 37.4 Evidence of gas hydrates in exploration wells Kg45-1 and Kj49-1 (see locations in Figs. 37.1, 37.2a), from Nimblett et al. (2005). At left, depth-converted seismic data on which well locations are marked; no BSR is recognised at either site. Boxes indicate gas hydrate zones (GHZ) identified from resistivity anomalies at right by Nimblett et al. (2005). Seismic and gamma ray logs together show the wells to have penetrated a thick mass transport deposit (MTD) at Kg45-1 and MTDs interbedded with channel-levee deposits at Kj49-1. At far right, the base of gas hydrate stability (BGHS) was calculated using CSMHYD assuming a phase boundary for 99% methane and 1% higher hydrocarbon in seawater of 34.5 ppt salinity and a geothermal gradient of 40 °C/km (Nimblett et al. 2005)

Mapping of pockmark-like seafloor features on the central Nile fan shows most to lie west of the BSR (Figs. 37.1, 37.2a), and to have distinctive positive morphologies that could be accounted for by near-surface gas hydrates (Fig. 37.5).

The distribution of pockmark-like features shown in Figs. 37.1 and 37.2 is that of 570 reflective patches 75–400 m wide, 410 mapped from a regional mosaic of multibeam imagery (25–100 m grids) and 160 from a dedicated local survey (see Fig. 37.5; Romer et al. 2014). The features are seen to be more abundant in the west, the vast majority lying beyond the area of the BSR in water depths of 1500–2700 m (Figs. 37.1, 37.2a). Seafloor studies in this area suggest that reflective patches correspond to areas of authigenic carbonate formed in response to a long-term (10^3 years) upward flux of methane, which continues to vent in some places (Fig. 37.5; Bayon et al. 2009b; Dupré et al. 2010; Römer et al. 2014). Subbottom profiles

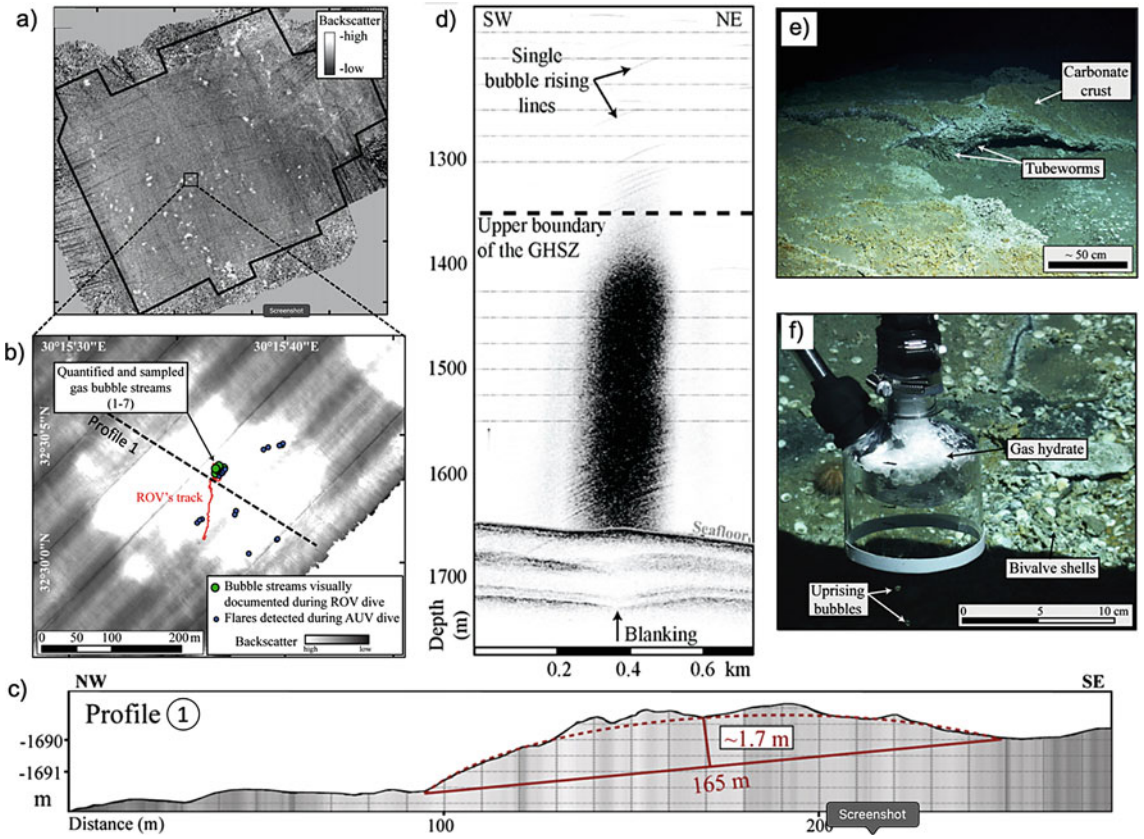

Fig. 37.5 Examples of pockmark-like seafloor seeps on the central Nile fan, from Römer et al. (2014): **a** ship-borne multibeam backscatter imagery over a 225 km^2 area (see Fig. 37.1) where 163 high-backscatter features were identified; **b** AUV-borne multibeam backscatter imagery showing details of gas venting from one feature; **c** NW–SE bathymetric profile along the dashed line in (**b**), showing the positive relief of the feature; **d** SW-NE Parasound profile across the same feature showing subsurface acoustic blanking and a water column gas flare 300 m high; **e** seafloor photo showing uplifted and fractured carbonate slabs over 0.5 m thick hosting chemosynthetic fauna (for location see green dots in (**b**)); **f** formation of gas hydrates during gas collection with an inverted funnel in the same area.

suggest that features above water depths of ≈1650–1950 m record vertical fluid migration through undeformed slope sediments (e.g., Fig. 37.5d), whereas those on the lower slope coincide with an area of superficial (<10 m) sediment deformation where fluids are inferred to migrate via inclined faults (Bayon et al. 2009b; Dupré et al. 2010; Dano et al. 2014; Migeon et al. 2014; Römer et al. 2014) and locally vertical pipes (Praeg et al. 2014). In general, seafloor seeps imply the upward migration of gas via conduits or fractures that cross the gas hydrate stability zone, a process that remains poorly understood but favours gas hydrate formation at depth and/or near the seafloor (e.g., Liu and Fleming 2007; Haacke et al. 2009; Riedel et al. 2010).

The reflective features of the central Nile fan are comparable in their sub-circular forms and dimensions to large pockmarks, but the vast majority are up to several metres high (e.g., Fig. 37.5c, d) and are found at the seafloor to comprise fractured carbonate slabs (Fig. 37.5e; Bayon et al. 2009b; Römer et al. 2014). The dating of a slab from the central Nile fan revealed downward cementation (Bayon et al. 2009a), supporting a model of self-sealing to drive the outward growth of wider pavements (Bayon et al. 2009b; Dupré et al. 2010). The stresses necessary to elevate and fracture carbonate slabs may be generated by gravity-driven sediment deformation (Bayon et al. 2009b) or by gas overpressure and/or gas hydrate formation (Römer et al. 2014; cf. Loher et al. 2018). It has been argued that large deep-sea pockmarks of complex morphology observed in other areas may be expressions of near-surface gas hydrate lenses, which form and dissolve in response to evolving patterns of upward fluid flow to drive phases of seafloor inflation and collapse (Sultan et al. 2010, 2014; Riboulet et al. 2016). The pockmark-like mounds of the central Nile fan may develop similarly above evolving gas hydrate lenses, driving vertical movements that fracture downward growing carbonate pavements to facilitate their upward stacking (Praeg et al. 2020).

37.4 Discussion: A Heterogeneous Gas Hydrate System

The Nile fan contains a gas hydrate system that is partially expressed by a discontinuous BSR, observed within an area of 6000 km^2, or one tenth of the deep-sea area lying within the MHSZ (Figs. 37.1, 37.2). The BSR indicates the presence within the fine-grained turbiditic sediments and MTDs of the Nile fan of a free gas zone of patchy distribution, above which gas hydrates are likely to occur (e.g., Majumdar et al. 2016). West of the BSR area, log data from two wells 45 km apart indicate the presence of gas hydrates in subsurface intervals 36–75 m thick near the base of the stability zone (Fig. 37.4). The wells lie in an area containing many seafloor seeps, but there is no indication that either lies near such a feature (Fig. 37.2a; Nimblett et al. 2005). These observations thus provide an example of a well-known phenomenon: that gas hydrates may be present over wide areas within deep marine sediments without everywhere giving rise to a BSR (e.g., Haacke et al. 2007; Majumdar et al. 2016; Hillman et al. 2017).

The BSR in this area is observed in two settings: (1) in the turbiditic fill of a series of fault-bound slope basins and (2) upslope of the basins in un-deformed sediments containing thick MTDs (Fig. 37.2). Linked variations in BSR depth and continuity within the basins offer evidence that both are influenced by upward fluid flow; in particular, the BSR is observed to rise towards seafloor while decreasing in amplitude toward the faults (Fig. 37.2b, c). Assuming no significant variations in sediment velocity or thermal conductivity within the basins, the observed decrease in BSR depth is consistent with higher heat transfer due to increased upward fluid flow near the faults (e.g., Riedel et al. 2010). Variations in the upward flow of gas-rich fluids have also been proposed to influence the continuity of BSRs, such that their appearance may be inhibited by a flux of dissolved gas that is too high to allow a free gas layer to be established beneath the stability zone (Haacke et al. 2007). Thus on the Nile fan, an increased upward flux of warm, gas-rich fluids could account for the fading of the BSR as it rises toward the faults (Fig. 37.2c).

At the scale of the central Nile fan, the area of the BSR contains few seafloor seeps, in contrast to an area to the west in which such features are abundant (Figs. 37.1, 37.2a). In the latter area (5000 km2), hundreds of pockmark-like mounds record the venting of microbially-derived methane, inferred to originate from relatively shallow depths within the fan (Gontharet et al. 2007; Bayon et al. 2009b; Romer et al. 2014). Different mechanisms have been proposed for the migration of gas through the hydrate stability zone (e.g., heat transfer, salt exclusion, hydrofracture), each involving enhanced upward fluid flow to drive the formation of chimney-like structures (e.g., Liu and Flemings 2007; Haacke et al. 2009; Riedel et al. 2010). Thus the increased density of gas vents westward across the central Nile fan (Figs. 37.1, 37.2a) could indicate higher overall rates of upward fluid flow than the area of the BSR to the east. As in the slope basins, this could be causal, the non-appearance of a BSR reflecting an upward flux of dissolved methane that is too high to establish a stable free gas layer at the base of the MHSZ (Haacke et al. 2007). An upward flux of methane-rich fluids would also be consistent with hydrate accumulation near the base of the stability zone between seepage structures (e.g., Liu and Flemings 2007; Hornbach et al. 2012), as indicated by wells in the same area (Fig. 37.4).

The central Nile fan thus contains a gas hydrate system expressed as two adjacent areas of comparable size but contrasting character (Fig. 37.2a): (1) an area featuring a discontinuous BSR and few gas vents, and (2) an area that contains abundant vents and downhole evidence of gas hydrates near the base of the stability zone but lacks a BSR. This heterogeneous character is hypothesised to reflect variations in upward fluid migration within the fan, with higher rates near faults and in areas of gas venting inhibiting BSR formation. Discontinuous or 'patchy' BSRs are observed in other deep-sea fans and have also been linked to variations in fluid flux, in most cases controlled by anticlinal structures of compressive or halokinetic origin (e.g., Hovland et al. 1997; Tanaka et al. 2003; Wu et al. 2007; Shedd et al. 2012; Morley et al. 2011, 2014). In these examples, BSR patches are correlated to enhanced fluid flux through faults to sustain seafloor fluid seeps. An interesting aspect of the central Nile fan gas hydrate system is that the opposite appears to be true; the BSR is anti-correlated to faults and to features of seafloor seepage, both of which are inferred to be associated with higher fluid flux.

The BSR and seepage areas together represent <20% of the area of the Nile fan within the MHSZ (Figs. 37.1, 37.2a). The full extent of the gas hydrate system is unknown. In the absence of a BSR, it has been speculated that gas hydrates may account for shallow diffractions that affect deeper seismic imaging in the western Nile fan at water depths of ≈1000–1500 m (Keggin et al. 2007), a depth range that includes the feather edge of the MHSZ. Some 300 km to the east, on the Nile fan offshore Israel, the presence of gas and gas hydrates has been argued to account for the scattered 3D seismic amplitude anomalies at water depths of 1300–1900 m, and for the formation of pockmarks above the edge of the MHSZ at water depths of 1000–1300 m (Tayber et al. 2019). The Nile fan is the upper part of a post-rift succession that contains seismic evidence of liquid and gaseous hydrocarbons at multiple levels, including near seafloor (Abdel et al. 2000, 2001; Loncke et al. 2004; Dupré et al.

2010), inferred to have migrated upward in response to overpressures generated by rapid Late Cenozoic deposition (Nashaat 1998; Dolson et al. 2005). In general, the migration of gas-rich fluids into the stability zone favours gas hydrate formation (Gornitz and Fung 1994; Liu and Fleming 2007; Hornbach et al. 2012), yet pore fluid expulsion may also act to inhibit the seismic expression of a BSR in passive margin depocentres (cf. Haacke et al. 2007). If this is indeed the case in the Nile fan, the gas hydrate system may extend over much of its deep-water extent. This possibility is of interest for the study of other large deep-sea fans that exhibit restricted or patchy BSRs but that may contain more extensive gas hydrate systems (e.g., the Niger delta (Hovland et al. 1997), the Amazon fan (Tanaka et al. 2003; Ketzer et al. 2018), the Mississippi fan (Shedd et al. 2012), the Pearl River Mouth basin (Wu et al. 2007)).

37.5 Outlook

The Nile deep-sea fan provides an interesting example of a deep-water gas hydrate system associated with widespread gas venting, offering a useful area to study the relation of such systems to fluid migration within passive margin depocenters. The heterogeneous characters of the gas hydrate system are suggested to be linked to spatial variations in fluid expulsion from the fan at different scales, which may inhibit BSR formation but favor gas hydrate formation over wide areas. This hypothesis invites testing through multi-disciplinary investigations to quantify near-surface fluid migration within the fan, and to understand the mechanisms by which gas is passing through the stability zone to vent to the ocean. The possibility that pockmark-like features of positive relief are expressions of near-surface gas hydrate lenses also invites testing, as the numbers observed across the central Nile fan would imply significant quantities of gas hydrates.

Acknowledgements D.P. acknowledges funding from the European Union's Horizon 2020 research and innovation program under Marie Skłodowska-Curie grant agreement no. 656821.

References

Abdel AA, El Barkooky A, Gerrits M et al (2000) Tectonic evolution of the Eastern Mediterranean Basin and its significance for hydrocarbon prospectivity in the ultradeepwater of the Nile Delta. Lead Edge 19(10):1041–1152. https://doi.org/10.1190/1.1438485

Abdel AA, El Barkooky A, Gerrits M et al (2001) Tectonic evolution of the eastern Mediterranean basin and its significance for the hydrocarbon prospectivity of the Nile Delta deepwater area. GeoArabia 6(3):363–384. https://pubs.geoscienceworld.org/geoarabia/article-pdf/6/3/363/4564261/aal.pdf

Bayon G, Loncke L, Dupré S et al (2009) Multi-disciplinary investigation of fluid seepage on an unstable margin: the case of the Central Nile Deep Sea Fan. Mar Geol 261:92–104. https://doi.org/10.1016/j.margeo.2008.10.00

Bayon G, Henderson GM, Bohn M (2009) U-Th stratigraphy of a cold seep carbonate crust. Chem Geol 260:47–56. https://doi.org/10.1016/j.chemgeo.2008.11.020

Caméra L, Ribodetti A, Mascle J (2010) Deep structures and seismic stratigraphy of the Egyptian continental margin from multichannel seismic data. Geol Soc, London, Special Publication 341(1):85–97. https://doi.org/10.1144/SP341.5

Dano A, Praeg D, Migeon S et al (2014) Fluid seepage in relation to seafloor deformation on the central Nile Deep-Sea Fan, part 1: evidence from sidescan sonar data. In: Krastel S et al (eds) Submarine mass movements and their consequences. 6th international symposium. Springer International, Advances in Natural and Technological Hazards Research 37:129–139. https://doi.org/10.1007/978-3-319-00972-8_12

Dolson JC, Boucher PJ, Siok J et al (2005) Key challenges to realizing full potential in an emerging giant gas province: Nile Delta/Mediterranean offshore, deep water, Egypt. In: Doré AG, Vining BA (eds) Petroleum geology: north-West Europe and global perspectives. Proceedings of the 6th petroleum geology conference, geological society, London, pp 607–624

Dupré S, Woodside J, Klaucke I et al (2010) Widespread active seepage activity on the Nile Deep Sea Fan (offshore Egypt) revealed by high-definition geophysical imagery. Mar Geol 275(1–4):1–19. https://doi.org/10.1016/j.margeo.2010.04.003

Finetti I, Morelli C (1973) Geophysical exploration of the Mediterranean Sea. Bollettino Di Geofisica Teorica Ed Applicata 15:263–341

Gennesseaux M, Burollet P, Winnock E (1998) Thickness of the Plio-Quaternary sediments (IBCM-PQ). Bolletino Di Geofisica Teorica Ed Applicata 39(4):243–284

Gontharet S, Pierre C, Blanc-Valleron MM et al (2007) Nature and origin of the diagenetic carbonate crusts and concretions from mud volcanoes and pockmarks of the Nile deep-sea fan (eastern Mediterranean sea). Deep-Sea Res II 54:1291–1316. https://doi.org/10.1016/j.dsr2.2007.04.007

Gornitz V, Fung I (1994) Potential distribution of methane hydrates in the world's oceans. Global Biogeochem Cy 8(3):335–347. https://doi.org/10.1029/94GB00766

Haacke RR, Westbrook GK, Hyndman RD (2007) Gas hydrate, fluid flow and free-gas: formation of the bottom-simulating reflector. Earth Planet Sci Lett 261:407–420. https://doi.org/10.1016/j.epsl.2007.07.008

Haacke RR, Hyndman RD, Park K-P et al (2009) Migration and venting of deep gases into the ocean through hydrate-choked chimneys offshore Korea. Geology 37:531–534. https://doi.org/10.1130/G25681A.1

Hillman JIT, Cook AE, Sawyer DE et al (2017) The character and amplitude of 'discontinuous' bottom-simulating reflections in marine seismic data. Earth Planet Sci Lett 459:157–169. https://doi.org/10.1016/j.epsl.2016.10.058

Hornbach MJ, Bangs NL, Berndt C (2012) Detecting hydrate and fluid flow from bottom simulating reflector depth anomalies. Geology 40(3):227–230. https://doi.org/10.1130/G32635

Hovland M, Gallagher W, Clennell MB et al (1997) Gas hydrate and free gas volumes in marine sediments: Example from the Niger Delta. Mar Pet Geol 14(3):245–255

Keggin J, Benson M, Rietveld W et al (2007) Multi-azimuth 3D provides robust improvements in Nile Delta seismic imaging. First Break 25(3):47–53. https://doi.org/10.3997/1365-2397.2007008

Ketzer JM, Augustin A, Rodriques F et al (2018) Gas seeps and gas hydrates in the Amazon deep-sea fan. Geo-Mar Lett 38(5):429–438. https://doi.org/10.1007/s00367-018-0546-6

Leithold EL, Blair NE, Wegmann KW (2016) Source-to-sink sedimentary systems and global carbon burial: a river runs through it. Earth Sci Rev 153:30–42. https://doi.org/10.1016/j.earscirev.2015.10.011

Liu X, Flemings PB (2007) Dynamic multiphase flow model of hydrate formation in marine sediments. J Geophys Res 112:B03101. https://doi.org/10.1029/2005JB004227

Loher M, Marcon Y, Pape T et al (2018) Seafloor sealing, doming and collapse associated with gas seeps and authigenic carbonate structures at Venere mud volcano, Central Mediterranean. Deep-Sea Res Part 1 137:76–96.https://doi.org/10.1016/j.dsr.2018.04.006

Loncke L, Gaullier V, Bellaiche G et al (2002) Recent depositional pattern of the NDSF from echo-character mapping. Interactions between turbidity currents, mass-wasting processes and tectonics. AAPG Bulletin 86:1165–1186

Loncke L, Mascle J, Parties FS (2004) Mud volcanoes, gas chimneys, pockmarks and mounds in the Nile deep-sea fan (Eastern Mediterranean): geophysical evidences. Mar Pet Geol 21(6):669–689. https://doi.org/10.1016/j.marpetgeo.2004.02.004

Loncke L, Gaullier V, Mascle J et al (2006) The Nile deep-sea fan: an example of interacting sedimentation, salt tectonics, and inherited subsalt paleotopographic features. Mar Pet Geol 23:297–315. https://doi.org/10.1016/j.marpetgeo.2006.01.001

Loncke L, Gaullier V, Droz L et al (2009) Multi-scale slope instabilities along the Nile deep-sea fan, Egyptian margin: a general overview. Mar Pet Geol 26(5):633–646. https://doi.org/10.1016/j.marpetgeo.2008.03.010

Lykousis V, Alexandri S, Woodside J et al (2009) Mud volcanoes and gas hydrates in the Anaximander mountains (Eastern Mediterranean Sea). Mar Pet Geol 26(6):854–872. https://doi.org/10.1016/j.marpetgeo.2008.05.002

Majumdar U, Cook AE, Shedd W et al (2016) The connection between natural gas hydrate and bottom-simulating reflectors. Geophys Res Lett 43:7044–7051. https://doi.org/10.1002/2016GL069443

Mascle J, Loncke L, Caméra L (2005) Geophysical evidences of fluid seepages and mud volcanoes on the Egyptian continental margin (Eastern Mediterranean). Bollettino Della Società Geologica Italiana, Volume Speciale 4:127–134

Mascle J, Mascle G (2012) Geological and morpho-tectonic map of the mediterranean domain, 1st edition. Commission for the Geological Map of the World, CGMW/UNESCO, Paris

Merey Ş, Longinos SN (2018) Numerical simulations of gas production from Class 1 hydrate and Class 3 hydrate in the Nile Delta of the Mediterranean Sea. J Nat Gas Sci Eng 52:248–266. https://doi.org/10.1016/j.jngse.2018.01.001

Migeon S, Ceramicola S, Praeg D et al (2014) Post-failure processes on the continental slope of the Central Nile Deep-Sea Fan: interactions between fluid seepage, creeping and sediment wave construction. In: Krastel S et al (eds) Submarine mass movements and their consequences. 6th international symposium. Springer International. Adv Nat Technol Hazards Res 37(11):117–127. https://doi.org/10.1007/978-3-319-00972-8_11

Minshull TA, Marín-Moreno H, Betlem P et al (2020) Hydrate occurrence in Europe: a review of available evidence. Mar Pet Geol 111:735–764. https://doi.org/10.1016/j.marpetgeo.2019.08.014

Morley CK, King R, Hillis R et al (2011) Deepwater fold and thrust belt classification, tectonics, structure and hydrocarbon prospectivity: a review. Earth Sci Rev 104:41–91. https://doi.org/10.1016/j.earscirev.2010.09.010

Morley CK, Warren J, Tingay M et al (2014) Comparison of modern fluid distribution, pressure and flow in sediments associated with anticlines growing in deepwater (Brunei) and continental environments (Iran). Mar Pet Geol 51:210–229. https://doi.org/10.1016/j.marpetgeo.2013.11.011

Nashaat M (1998) Abnormally high fluid pressure and seal impacts on hydrocarbon accumulations in the Nile Delta and North Sinai Basins, Egypt. In: Law BE, Ulmishek GF, Slavin VI (eds) Abnormal pressures in hydrocarbon environments. AAPG Memoir 70:161–180

Newton CS (2006) Importance of mass transport complexes in the development of the central and western quaternary Nile Fan. Unpublished MSc thesis, Dalhousie University, Halifax, Nova Scotia, Canada, p 122

Nimblett JN, Shipp RC, Strijbos F (2005) Gas hydrate as a drilling hazard: examples from global deepwater settings. Offshore Technology Conference, Houston, Texas, USA. OTC 17476, p 7. https://doi.org/10.4043/17476-MS

Nott JA, Gibson JL, Shipp RC (2001) Near-surface depositional framework of the northeastern Mediterranean (NEMED) concession area, deepwater Egypt. AAPG Annual Meeting, Denver, CO, USA; AAPG Search and Discovery Article #90906. http://www.searchanddiscovery.com/abstracts/html/2001/annual/abstracts/0570.htm

Omeru T, Cartwright JA (2015) Multistage, progressive slope failure in the Pleistocene pro-deltaic slope of the West Nile Delta (Eastern Mediterranean). Mar Geol 362:76–92. https://doi.org/10.1016/j.margeo.2015.01.012

Pape T, Kasten S, Zabel M et al (2010) Gas hydrates in shallow deposits of the Amsterdam mud volcano, Anaximander Mountains, Northeastern Mediterranean Sea. Geo-Mar Lett 30:187–206. https://doi.org/10.1007/s00367-010-0197-8

Praeg D, Geletti R, Mascle et al (2008) Geophysical exploration for gas hydrates in the Mediterranean Sea and a bottom-simulating reflection on the Nile Fan. Gruppo Nazionale di Geofisica della Terra Solida, GNGTS 27° Convegno Nazionale, Trieste, Italy. Riassunti Estesi, pp 467–469. http://www3.ogs.trieste.it/gngts/files/2008/S32/Riassunti/32-prae.pdf

Praeg D, Geletti R, Wardell N et al (2011) The Mediterranean Sea: a natural laboratory to study gas hydrate dynamics? In: Proceedings of the 7th international conference on gas hydrates (ICGH7 2011), Edinburgh, Scotland, UK, 17–21 July 2011; Full Paper 00322, p 8. https://hal.archives-ouvertes.fr/hal-03315746

Praeg D, Ketzer JM, Augustin AH et al (2014) Fluid seepage in relation to seabed deformation on the central Nile Deep-Sea Fan, part 2: evidence from multibeam and sidescan imagery. In: S. Krastel et al (eds) Submarine mass movements and their consequences, 6th international symposium. Springer International. Adv Nat Technol Hazards Res 37:141–150. https://doi.org/10.1007/978-3-319-00972-8_13

Praeg D, Migeon S, Dano A et al (2020) Positive-relief carbonate pavements on the central Nile deep-sea fan: gas hydrate blisters or carbonate-filled pockmarks? Pockmarks et Ecosystèmes Benthiques, Société Géologique de France, Paris. Livre des Résumés, p 6. https://sgf-pockmarks.sciencesconf.org/browse/speaker?authorid=786882

Prinzhofer A, Deville E (2013) Origins of hydrocarbon gas seeping out from offshore mud volcanoes in the Nile delta. Tectonophysics 591:52–61. https://doi.org/10.1016/j.tecto.2011.06.028

Riboulet V, Sultan N, Imber P et al (2016) Initiation of gas-hydrate pockmark in deep-water Nigeria: geo-mechanical analysis and modelling. Earth Planet Sci Lett 434:252–263. j.epsl.2015.11.047

Riedel M, Tréhu AM, Spence GD (2010) Characterizing the thermal regime of cold vents at the northern Cascadia margin from bottom-simulating reflector distributions, heat-probe measurements and borehole temperature data. Mar Geophys Res 31:1–16. https://doi.org/10.1007/s11001-010-9080-2

Römer M, Sahling H, Pape T et al (2014) Methane fluxes and carbonate deposits at a cold seep area of the Central Nile Deep Sea Fan, Eastern Mediterranean Sea. Mar Geol 347:27–42. https://doi.org/10.1016/j.margeo.2013.10.011

Rowan MG, Peel FJ, Vendeville BC (2004) Gravity-driven fold-belts on passive margins. In: McKay KR (ed) Thrust tectonics and hydrocarbon systems. AAPG Memoir 82:157–182

Sharaf El Din H (2006) Recent exploration of methane hydrate on the continental shelf of Egyptian Mediterranean coast. In: 5th international workshop on methane hydrate research & development, 9–12 October, Edinburgh, Scotland, UK

Sharaf El Din SH, Nassar M (2010) Gas hydrates over the Egyptian Mediterranean coastal waters. European Geosciences Union General Assembly, Vienna Austria; Geophysical Research Abstracts 12: EGU2010–78. https://meetingorganizer.copernicus.org/EGU2010/EGU2010-78.pdf

Shedd W, Boswell R, Frye M et al (2012) Occurrence and nature of "bottom simulating reflectors" in the northern Gulf of Mexico. Mar Pet Geol 34(1):31–40. https://doi.org/10.1016/j.marpetgeo.2011.08.005

Sultan N, Marsset B, Ker S et al (2010) Hydrate dissolution as a potential mechanism for pockmark formation in the Niger delta. J Geophys Res 115:B08101. https://doi.org/10.1029/2010JB007453

Tassy A, Crouzy E, Gorini C et al (2015) Egyptian Tethyan margin in the Mesozoic: evolution of a mixed carbonate-siliciclastic shelf edge (from Western Desert to Sinai). Mar Pet Geol 8:565–581. https://doi.org/10.1016/j.marpetgeo.2015.10.011

Tayber Z, Meilijson A, Ben-Avraham Z et al (2019) Methane hydrate stability and potential resource in the Levant basin, southeastern Mediterranean Sea. Geosciences 9(7):306. https://doi.org/10.3390/geosciences9070306

Vandré C, Cramer B, Gerling P et al (2007) Natural gas formation in the western Nile delta (Eastern Mediterranean): thermogenic versus microbial. Organ Geochem 38:523–539. https://doi.org/10.1016/j.orggeochem.2006.12.006

Wu S, Wang X, Wong HK et al (2007) Low-amplitude BSRs and gas hydrate concentration on the northern margin of the South China Sea. Mar Geophys Res 28:127–138. https://doi.org/10.1007/s11001-007-9020-y